

Nature of the Water Structure inside the Pools of Reverse Micelles Sensed by Laser-Induced Optoacoustic Spectroscopy[†]

Claudio D. Borsarelli and Silvia E. Braslavsky*

Max-Planck-Institut für Strahlenchemie, Postfach 10 13 65, D-45413 Mülheim an der Ruhr, Germany

Received: April 7, 1997; In Final Form: May 22, 1997[©]

Reaction volume changes, ΔV_R , enthalpy content, ΔH_{MLCT} , and decay lifetimes, τ_2 , of the metal-to-ligand charge transfer (MLCT) complex of (2,2'-bipyridine)tetracyanoruthenate(II) complex, $Ru(bpy)(CN)_4^{2-}$, inside the water pools of sodium bis(2-ethylhexyl)sulfosuccinate (AOT) reverse micelles dispersed in *n*-alkanes, were determined using laser-induced optoacoustic spectroscopy (LIOAS). Emission quantum yields, Φ_{em} , of the complex were also determined by steady-state measurements. The enthalpy content of the MLCT state of $Ru(bpy)(CN)_4^{2-}$ was not dependent on the amount of water inside the reverse micelles (defined as the molar ratio $R = [H_2O]/[AOT]$) and was, within experimental error, similar to that in water. However, the values of τ_2 and Φ_{em} decrease while those of ΔV_R increase as the values of R are incremented from 3 to 10. At the larger R values, τ_2 , Φ_{em} , and particularly ΔV_R resemble the values in neat water. These results are interpreted to arise from the type of water involved in the hydrogen bond interactions between the cyanide ligands of the complex and the water molecules (second-sphere donor–acceptor interactions). In this framework, for reverse micelles solutions at $R \geq 10$, the hydrogen bonds are made with the “free” water in the inner pool. For $R < 10$ the properties of $Ru(bpy)(CN)_4^{2-}$ are indicative of a more rigid microenvironment in the micellar core. Thus, the photophysical properties (and particularly ΔV_R) of $Ru(bpy)(CN)_4^{2-}$ are very sensitive to its microenvironment and serve as a probe of the type of water involved in the hydrogen bonding. A combination of the LIOAS data from temperature-dependent measurements in neat water with those for the same complex in reverse micelles dispersed in various *n*-alkanes at high R values improved in 1 order of magnitude the accuracy of the ΔH_{MLCT} and ΔV_R values for the MLCT state.

Introduction

The reaction volume changes associated with the intramolecular photooxidation of Ru(II) in bipyridine cyano complexes, obtained by laser-induced optoacoustic spectroscopy (LIOAS), were attributed to photoinduced changes in the hydrogen bond strength (specific interactions) between the cyano ligands and the water molecules of the first solvation shell. In particular, the values determined for the formation of the MLCT state in the homologous series $Ru(bpy)(CN)_4^{2-}$, $Ru(bpy)(CN)_3(CNCH_3)^-$, and $Ru(bpy)(CN)_2(CNCH_3)_2$, which are expansions for the first two compounds (*i.e.*, the molar structural volume change is $\Delta V_R = 15, 10$, and *ca.* 0 cm³/mol), directly correlated with the number of cyanide ligands available for donor–acceptor interactions with water.¹ In a further investigation of photoinduced volume changes by LIOAS we attributed the contraction of *ca.* 10 cm³/mol, observed upon production of the triplet state of 5,10,15,20-tetrakis-(4-sulfophenyl)porphyrin in basic solutions, to a stronger hydrogen bond in the triplet state from the central N atoms in the porphyrin ring to the water molecules.² On the basis of the concept that changes in the hydrogen-bonding ability of the compounds are largely responsible for the transient reaction volume changes determined using LIOAS in aqueous media,³ we decided to analyze a system in which it is possible to vary the type of water available for such a hydrogen bond.

Reverse micelles are an ideal system for the purpose outlined. They are thermodynamically stable “water-in-oil” microemulsions, consisting of nanometer-sized water droplets dispersed

in a nonpolar solvent and stabilized by surfactant molecules and with a peculiar molecular heterogeneity caused by the amphiphilic nature of the surfactant that resides in an interface between water and the nonpolar solvent. Three different compartments are available for the localization of small solutes: (a) the internal aqueous core or water pool, (b) the micellar interface formed by a monolayer of surfactant molecules with their polar head groups oriented toward the water pool, and (c) the external organic phase.^{4,5}

The internal aqueous core presents inhomogeneous properties and is considered as a sphere with radially varying polarity and viscosity.⁶ These properties are a function of the molar ratio of water to the surfactant.^{6,7} In particular, for sodium bis(2-ethylhexyl)sulfosuccinate (Aerosol OT, AOT) as a surfactant and a molar ratio of water to AOT of $R = [H_2O]/[AOT] \geq 10$, the formation of a water pool with “free” water molecules at the center of the micelle is expected, with properties similar to those of pure water. For lower R values, most of the water molecules are immobilized *via* hydration of the sodium counterions and the ionized polar head groups of AOT.^{6,8}

An additional interest in studying weak interactions such as hydrogen bonds inside reverse micelles resides in the fact that the highly structured water molecules in the reverse micelles can be thought of as primitive models of the water molecules in biological systems.^{4,5,9,10}

$Ru(bpy)(CN)_4^{2-}$ (Figure 1) is a suitable compound for our studies since it exhibits a long-lived, light-emitting metal-to-ligand charge transfer (MLCT, $d_{Ru} \rightarrow \pi^*_{bpy}$) state, which in the absence of quenchers fully returns to the ground state in 100 ns.¹¹ The Ru(II) center, oxidized upon excitation to the MLCT state, is strongly coupled with polar solvents through the cyanide ligands by second-sphere donor–acceptor interactions, while the bipyridine ligand (which is reduced on MLCT

[†] Dedicated to Professor Eduardo A. Lissi on the occasion of his 60th birthday. Work reported at the XVth IUPAC Symposium on Photochemistry, Helsinki, July 1996.

* To whom correspondence should be addressed.

[©] Abstract published in *Advance ACS Abstracts*, July 1, 1997.

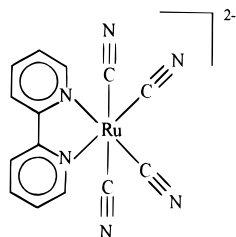


Figure 1. The $\text{Ru}(\text{bpy})(\text{CN})_4^{2-}$ complex.

formation) is free from specific solvation effects, due to its delocalized electronic cloud and to its hydrophobic character.¹¹ The anionic character of the complex ensures its solubilization inside the water pool of the AOT reverse micelles.

LIOAS has been successfully applied in aqueous and non-aqueous homogeneous media using different protocols in order to separate the thermal (ΔV_{th}) from the reaction (ΔV_{R}) contributions to the total volume change, which in turn produces the detected pressure wave.^{3,12–18} In aqueous solutions the two contributions to the pressure wave are separated by temperature-dependent measurements, taking advantage of the fact that the cubic expansion coefficient β (to which only ΔV_{th} is proportional) of water strongly depends on temperature.^{12,13,17,18} However, the thermoelastic parameters of nonaqueous media exhibit a poor dependence on temperature. In this case, the ΔV_{R} values have been determined by using a series of homologous solvents with variable thermoelastic parameters.^{14–16,18} Thus, for our purposes AOT is the ideal surfactant since it solubilizes large amounts of water in which $\text{Ru}(\text{bpy})(\text{CN})_4^{2-}$ can be dissolved and produces well-shaped aggregates in several nonpolar solvents,¹⁹ which makes possible the variation of the thermoelastic parameters of the medium.

There are only few LIOAS studies in microheterogeneous media. Herman and Goodman determined the enthalpy and ΔV_{R} values upon photodecomposition of diphenylcyclopropenone (DPCP) by temperature-dependent LIOAS experiments in aqueous micelles of sodium dodecyl sulfate (SDS) and cetyl trimethyl ammonium chloride (CTAC).¹⁷ The results in micellar media were different from those for the same reaction in a series of alkanes at constant temperature.¹⁴ This controversy has recently been analyzed by Schmidt and Schütz¹⁸ who compared the photodecomposition of DPCP in alkanes and in SDS micelles, using both protocols for the variation of the thermoelastic parameters of the media. Similar enthalpy and ΔV_{R} values were found for this reaction, regardless of the medium and in agreement with the previously obtained values in alkanes.¹⁴ The reported discrepancy¹⁷ was attributed to an incorrect procedure for the estimation of the thermoelastic parameters of the micellar solutions and for the determination of the reaction quantum yield.¹⁸ Thus, the correct estimation of the thermoelastic parameters in the medium under study plays a central role in LIOAS experiments.

In reverse micelles, LIOAS has only been employed for the determination of the intersystem crossing and singlet oxygen generation quantum yields of rose bengal dissolved in AOT–water–isooctane solutions.²⁰ Advantage was taken of the fact that the LIOAS sensitivity in organic medium is larger than in aqueous solutions, primarily because β is larger in every nonaqueous medium than in water, thus increasing the signal amplitude.²⁰ We are not aware of determinations of ΔV_{R} values in reverse micelles. Due to the contribution of the ΔV_{R} term to the total pressure wave generated after pulse excitation, it is important to quantitatively evaluate this effect in order to properly derive the enthalpy levels of the photoinduced products.

In this paper we report the enthalpy content and volume changes associated with the MLCT state of $\text{Ru}(\text{bpy})(\text{CN})_4^{2-}$,

as well as its decay lifetime, derived from a LIOAS study in AOT–water–*n*-alkanes solutions (from *n*-hexane to *n*-dodecane), at several *R* values ($3 \leq R \leq 20$). The determination of the thermoelastic parameters of the AOT reverse micelles solutions is described in detail.

Experimental Section

Materials. (2,2'-Bipyridine)tetracyanoruthenate (II), $\text{Ru}(\text{bpy})(\text{CN})_4^{2-}$, as its potassium salt, was supplied by Professor Franco Scandola (Ferrara). Its synthesis has been already published.^{1,11} The calorimetric references ferrocene (Aldrich) for pure alkanes and Ni(II) perchlorate (Fluka) for water pools of reverse micelles were used as received. Sodium bis(2-ethylhexyl)sulfosuccinate (AOT, Sigma) was used without further purification. The alkane solvents (*n*-hexane, *n*-heptane, *n*-octane, *n*-nonane, *n*-decane, *n*-undecane, and *n*-dodecane; all from Merck) were purified before use in various ways, *i.e.*, by distillation, by column chromatography, or by preparative gas chromatography. Water was deionized.

Preparation of the Solutions. A 0.1 M solution of AOT was prepared in the appropriate alkane solvent. Subsequently, 10 μL of an aqueous stock of suitable concentration of the sample or reference compound were injected to 3 mL of the surfactant solution. The final *R* values were adjusted with neat water. The mixture was shaken or mildly sonicated for a few minutes until a visually clear solution was obtained. The concentration of $\text{Ru}(\text{bpy})(\text{CN})_4^{2-}$ was *ca.* 2×10^{-5} M. Under these conditions and taking into account the aggregation number of AOT in each solvent,¹⁹ the sample to micelles molar ratio was always < 0.1 .

Methods. The absorbances of reference and sample solutions were recorded with a Shimadzu UV-2102PC spectrophotometer and matched within 5% at 400 nm. The LIOAS setup has been already described.^{1,13} Excitation was with a 15 ns (fwhm) laser pulse at 400 nm produced by an Excimer laser (FL2000 Lambda Physik, XeCl)-pumped dye laser (EMG 101 MSC and with Furan 2 as dye). A 40 μm poly(vinylidene fluoride) film was used as acoustic detector. The signals were amplified 100 times (Comlinear E103) and fed into a transient recorder (Tektronix TDS 684A, operating at 1 Gs/s and averaging 200/300 signals). The acoustic transit time was 120 ns which allowed for a time resolution of 10–15 ns using deconvolution techniques.^{1,3,16} The solutions of $\text{Ru}(\text{bpy})(\text{CN})_4^{2-}$ were deoxygenated by Ar-bubbling for 15–20 min with solvent-saturated Ar. Temperature was $(25.0 \pm 0.1)^\circ\text{C}$. No photobleaching of the sample or the reference solutions was detected after each experiment.

Steady-state emission spectra were performed with a Spex Fluorolog spectrofluorometer in deoxygenated solutions. The emission quantum yields, Φ_{em} , of $\text{Ru}(\text{bpy})(\text{CN})_4^{2-}$ in AOT solutions were calculated by comparing the spectrally integrated emission in the AOT solution with that of $\text{Ru}(\text{bpy})(\text{CN})_4^{2-}$ in pure water ($\Phi_{\text{em}} = 0.0068$),²¹ after correcting for the difference in refractive index of the solvents.

LIOAS Signal Handling. The procedures used for the LIOAS signal analysis have been described in several publications.^{1–3,16} Deconvolution techniques are required for a detailed description of the time evolution of the slower pressure release when transient species are produced with lifetimes within the acoustic transient time. The signal of the sample is regarded as a convolution of the instrumental response (obtained with a calorimetric reference) and a time-dependent multiexponential decay function describing the pressure behavior in the sample after laser excitation. The reference signal depends only on the heat release multiplied by the thermal expansivity of the solvent [defined as the ratio $(\beta/c_p\rho)$, where $\beta = (\partial V/\partial T)_P$ ($1/V$)

is the cubic expansion coefficient, c_p is the heat capacity at constant pressure, and ρ is the mass density of the medium], while the sample signal might have an extra contribution from structural volume changes $\Delta V_r = n\Phi_R\Delta V_R$ (ΔV_r is the total structural contribution of the volume change to the signal, n is the number of Einsteins absorbed, and Φ_R is the reaction quantum yield), which does not depend on the thermal expansivity. Thus, assuming that the thermal and the structural contributions to the pressure wave show the same time behavior, the recovered amplitudes of the multiexponential function of the sample, φ_i , normalized with respect to the amplitude of the reference compound ($\varphi = 1$), are given by eq 1,^{1,2,16}

$$E_\lambda \varphi_i = q_i + \Phi_{R,i} \Delta V_{R,i} (c_p \rho / \beta) \quad (1)$$

where E_λ is the excitation energy per absorbed Einstein (299.3 kJ/mol at 400 nm), q_i stands for the heat released in the particular relaxation process, $\Phi_{R,i}$ is the quantum yield, and $\Delta V_{R,i}$ is the volume change per mole of the i th step. Signal analysis was performed using the Sound Analysis version 1.13 software (Quantum Northwest), and the amplitude and lifetime values were obtained by averaging from two series of measurements at three different fluence values for each solution. This procedure yields errors lower than 5 and 10% for the LIOAS amplitudes and lifetimes, respectively. The lifetimes present more scattering probably due to some variation in the deoxygenation procedure of the solutions.

Thermoelastic Properties of the AOT Solutions in n -Alkanes. For a correct application of eq 1 in AOT solutions, it is necessary to estimate the value of the $(c_p \rho / \beta)$ ratio in each medium by comparing the LIOAS signal amplitude in a medium with known thermoelastic properties to those in the medium under study.^{13,22} For this purpose, the LIOAS signals of a calorimetric reference in each pure alkane (the reference solvents, with tabulated thermoelastic properties)²³ were compared with those in the AOT dispersions in the respective alkane, and eq 2 was used

$$(c_p \rho / \beta)_{RM} = \frac{H_{alk}^n (\kappa_T)_{alk}}{H_{RM}^n (\kappa_T)_{RM}} (c_p \rho / \beta)_{alk} \quad (2)$$

where H^n is the fluence-normalized signal amplitude, κ_T is the isothermal compressibility, and the subscripts alk and RM refer to alkane and AOT reverse micelles media, respectively.

Since $\text{Ru}(\text{bpy})(\text{CN})_4^{2-}$ is expected to be localized in the water pool of the AOT micelles, it was necessary to employ two different calorimetric references: a water soluble compound for the water pool and a hydrophobic reference for the pure alkanes. $\text{Ni}(\text{ClO}_4)_2$ and ferrocene, respectively, were selected for this purpose, in view of their large absorbance at 400 nm (the excitation wavelength). The absorption spectra of $\text{Ni}(\text{ClO}_4)_2$ in AOT solutions at different R were identical to the spectrum in water. Ferrocene showed the same absorption spectrum in all n -alkanes. In order to test that both references release all the absorbed energy into the medium as heat, the normalized signal amplitudes for each reference in pure solvent at the same temperature and absorbance were compared.¹⁸ The absorbed-fluence dependence of the amplitude, H , for $\text{Ni}(\text{ClO}_4)_2$ in water (open squares) and for ferrocene in n -decane (filled squares) are shown in Figure 2. Using the tabulated data for κ_T , β , ρ , and c_p for both solvents at 25 °C²³ and eq 2, the measured and calculated H_w^n/H_{alk}^n ratios agree within 7%, which validates the use of these substances as calorimetric references.

The fluence dependences of H for $\text{Ni}(\text{ClO}_4)_2$ in AOT–water– n -decane solutions at $R = 5$ and 20 are also depicted in Figure

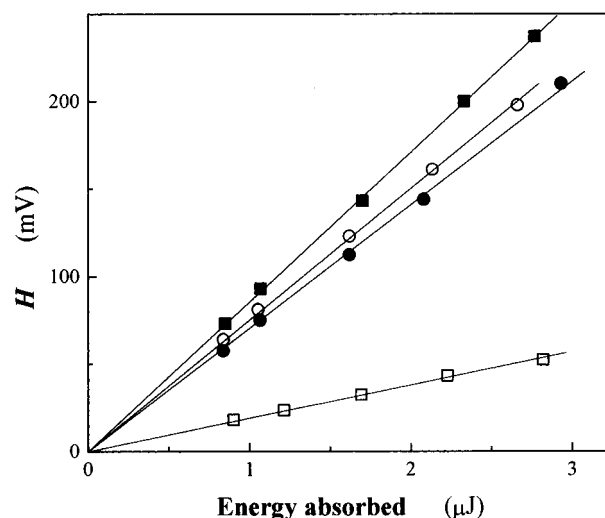


Figure 2. LIOAS signal amplitude, H , as function of the absorbed fluence for the calorimetric references in homogeneous and reverse micelles solutions: (■) ferrocene in n -decane and $\text{Ni}(\text{ClO}_4)_2$ in (□) water, (○) AOT–water– n -decane at $R = 5$, and (●) AOT–water– n -decane at $R = 20$.

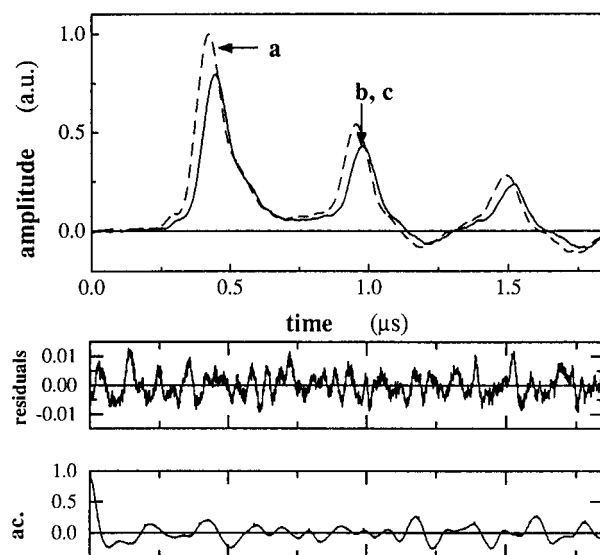


Figure 3. LIOAS signals for the calorimetric reference ferrocene in n -heptane (curve a) and $\text{Ni}(\text{ClO}_4)_2$ in AOT–water– n -heptane at $R = 10$ (curve b) together with the fit (curve c), residuals, and autocorrelation waveforms, after deconvolution using a monoexponential decay function and the ferrocene signal as reference. $\varphi = 0.801$, $\tau = 5$ ns, $\chi^2 = 1.57 \times 10^{-5}$. Note that the fitted curve completely coincides with the measured signal from the sample.

2. The signal amplitudes in AOT solutions are lower than in the respective neat alkane, and they decrease with increasing R . A similar effect was observed using o -hydroxybenzophenone (OHBP) as calorimetric reference in AOT–isooctane solutions.²⁰ This effect was attributed to the increment of water in the microemulsion, which results in a smaller thermal expansivity (to which the signal is directly proportional), mainly because $\beta_w < \beta_{alk}$.

The LIOAS signal maxima for $\text{Ni}(\text{ClO}_4)_2$ in AOT microemulsions are shifted to longer times with respect to that for ferrocene in neat n -alkanes. This effect is shown in Figure 3 for AOT– n -heptane dispersions at $R = 10$.

Satisfactory fits of the LIOAS signal from $\text{Ni}(\text{ClO}_4)_2$ in AOT microemulsions were obtained using as a reference the signals from ferrocene dissolved in the corresponding alkane and a monoexponential decay function. The program freely adjusted

two parameters. In all cases a fast decay time (< 8 ns) was found with an amplitude value similar to the energy-normalized signal amplitudes ratio, $H_{\text{RM}}^n/H_{\text{alk}}^n$, as derived from Figure 2. This result indicates that $\text{Ni}(\text{ClO}_4)_2$ releases all the absorbed energy as heat into the solution in a time shorter than the time resolution of our experiment. The use of Ni^{2+} salts as calorimetric references recently found support by a transient lens study showing that deactivation of the excited cation takes place in a time shorter than 500 ps.²⁴ In addition, it has also been recently shown that in AOT reverse micelles at $R \leq 10$, the heat release from the water pool to the organic solvent is so rapid that the acoustic wave is generated as if it were from a reference solution with an homogeneous distribution of the excited species. At larger R values the thermal diffusion was estimated to be within 1–10 ns, which is still faster than our time resolution.²⁵

The difference in the signal arrival time of the LIOAS signal to the detector for the references is an indication of differences in the sound velocity and consequently, in the isothermal compressibility of the medium, κ_T .^{18,22} κ_T is related to the adiabatic compressibility of the solution κ_S by eq 3²⁶

$$\kappa_T = \kappa_S + \theta = \frac{1}{\rho \nu_a^2} + T \frac{\beta^2}{c_p \rho} \quad (3)$$

where ν_a is the sound velocity and T is the absolute temperature. In aqueous solutions, the θ ratio is negligible at the normal temperatures and $\kappa_T \approx \kappa_S$. However, in alkanes at room temperature, θ contributes 10–20% to κ_T .²³ This difference exceeds the LIOAS experimental error (ca. 5–10%), and the term θ should be considered. A decrease of the θ ratio in AOT media relative to that in neat alkanes is expected, due to the larger value of ρ and the fact that the addition of water reduces the value of β (*vide supra*). However, since β and c_p in AOT dispersions are not known, it is necessary to estimate the value of θ in AOT microemulsions. A rough estimation of the decrease in θ can be made by considering $\theta_{\text{RM}} = f_{\text{alk}} \theta_{\text{alk}}$, where f_{alk} is the mass fraction of the alkane in the micellar dispersion, which mainly depends on R if the surfactant concentration is constant. Under our experimental conditions with $[\text{AOT}] = 0.1$ M and $3 \leq R \leq 20$, the f_{alk} values are between ca. 0.95 and 0.89, respectively. Thus, the κ_T values in AOT solutions were estimated using eq 3 with ρ and ν_a measured for each dispersion and the calculated value of θ in reverse micelles solutions. The value of ν_a was obtained by comparing the arrival time of the first maximum of the LIOAS signal of the references in the AOT solution and in pure alkane. The mass density of the AOT solutions at different R values and alkanes were determined by weighing the solutions in 2 mL calibrated flasks. The procedure was repeated 5–6 times for each solution, and the values obtained were within $\pm 5\%$.

The values of $(c_p \rho / \beta)$ ratio calculated for the AOT microemulsions using eq 2 for each organic solvent at $R = 5, 10, 20$ are presented in Figure 4 as a function of the length of the hydrocarbon, together with the values of the $(c_p \rho / \beta)$ for the pure alkanes as obtained from the literature.²³

Results

The UV–vis spectra of $\text{Ru}(\text{bpy})(\text{CN})_4^{2-}$ in AOT–water– n -alkane solutions were the same for all R values (spectra not shown). The position of the MLCT absorption maxima at 400 nm, the width of the absorption band extending from 350 to 450 nm, and the absorbances ratio between maxima were identical to those in pure water.^{11,21} The corrected emission maximum wavelength for $\text{Ru}(\text{bpy})(\text{CN})_4^{2-}$ in AOT solutions

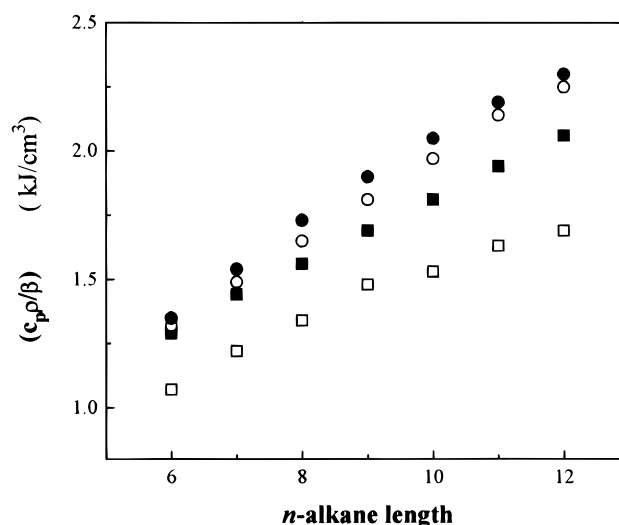


Figure 4. Ratio of thermoelastic parameters ($c_p \rho / \beta$) vs the n -alkane length: (\square) neat alkanes (from left to right n -hexane, n -heptane, n -octane, n -nonane, n -decane, n -undecane, and n -dodecane), and in AOT reverse micelles dispersions with R (\blacksquare) 5, (\circ) 10, and (\bullet) 20. For the micelles, each value is the average of two independent measurements and the estimated error is $\pm 7\%$.

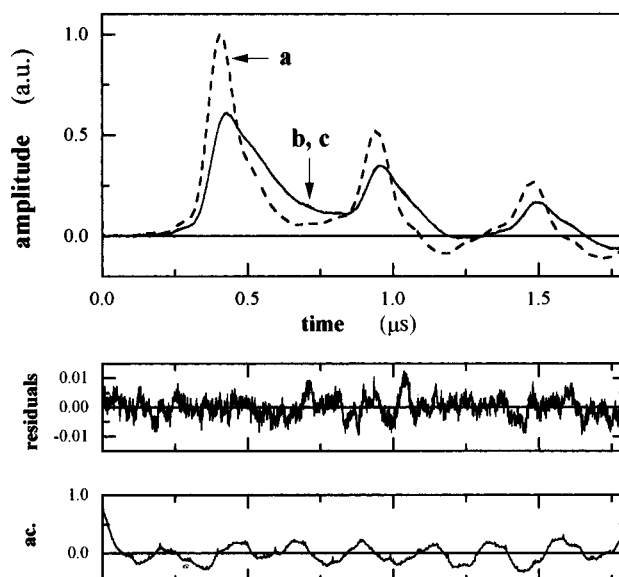


Figure 5. LIOAS signals for the reference $\text{Ni}(\text{ClO}_4)_2$ (curve a) and $\text{Ru}(\text{bpy})(\text{CN})_4^{2-}$ (curve b), in AOT–water– n -octane at $R = 20$ together with the fit (curve c), residuals, and autocorrelation waveforms, after deconvolution using a sequential biexponential decay function. $\varphi_1 = 0.325$, $\tau_1 = 1$ ns, $\varphi_2 = 0.681$, $\tau_2 = 117$ ns, $\chi^2 = 1.32 \times 10^{-5}$. Note that the fitted curve completely coincides with the measured signal for the sample.

(624 nm) was the same as that in neat water. However, the emission intensity decreased as R increased. At $R = 20$ the emission quantum yield ($\Phi_{\text{em}} = 0.0075$) had nearly the same value as that in pure water ($\Phi_{\text{em}} = 0.0068$)²¹ (see Table 1).

Figure 5 shows the LIOAS signal obtained for $\text{Ru}(\text{bpy})(\text{CN})_4^{2-}$ in AOT–water– n -octane at $R = 20$, together with that of the calorimetric reference $\text{Ni}(\text{ClO}_4)_2$. The shape of the sample signal is quite different from that of the reference. Satisfactory fits of the LIOAS signals of the sample were obtained using two sequential exponential decay functions (Figure 5). Allowing all four parameters (two lifetimes and two preexponential factors) to be varied freely, in all cases the program found two well-separated decay times: $\tau_1 < 1$ ns and τ_2 between 110 and 175 ns. The value of τ_1 is more or less arbitrary; it only means

TABLE 1: Structural Volume Change, ΔV_R , Enthalpy Content, ΔH_{MLCT} , Decay Lifetime, τ_2 , and Emission Quantum Yield, Φ_{em} , Associated with the MLCT State of Ru(bpy)(CN) $_4^{2-}$ in 0.1 M AOT–Water–*n*-Alkanes Reverse Micelles at Various Values of $R = [H_2O]/[AOT]$ and in Aqueous Solutions

solutions	ΔV_R MLCT formation (cm ³ /mol)	ΔV_R MLCT decay (cm ³ /mol)	ΔH_{MLCT} (kJ/mol)	τ_2^a (ns)	$\Phi_{em} (\times 10^2)$
0.1 M AOT; $R =$					
3	6.0 \pm 2.0	−7.0 \pm 2.5	221 \pm 6	162 \pm 12	1.08 \pm 0.05
5	8.1 \pm 1.0	−8.0 \pm 1.0	228 \pm 5	150 \pm 10	1.01 \pm 0.05
7	13.0 \pm 1.5	−12.7 \pm 2.0	225 \pm 5	138 \pm 10	0.94 \pm 0.05
10	15.5 \pm 1.0	−15.8 \pm 2.0	225 \pm 5	124 \pm 10	0.85 \pm 0.04
15	15.2 \pm 1.0	−15.6 \pm 1.5	230 \pm 7	119 \pm 10	0.78 \pm 0.04
20	15.4 \pm 1.0	−14.5 \pm 1.5	225 \pm 5	116 \pm 10	0.75 \pm 0.05
water ^b	15.3 \pm 0.9	−16.7 \pm 0.9	211 \pm 20	100 \pm 20	
water ^c	14.3 \pm 1.0	−14.0 \pm 1.0	218 \pm 20	104 \pm 10	0.68 ^d
water + 0.1 M AOT; $R = 20^e$	14.9 \pm 0.2	−15.2 \pm 0.2	228 \pm 2		

^a From LIOAS measurements. ^b See also ref 1. ^c This work. ^d From ref 21. ^e Combination of temperature-dependent measurements in water and in AOT reverse micelles at $R = 20$ dispersed in different *n*-alkanes, see Figure 7.

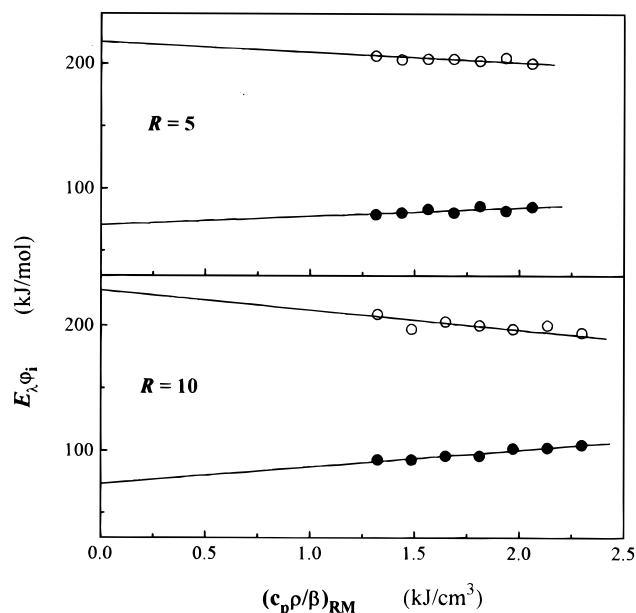


Figure 6. First and second amplitudes of the fitting function for the LIOAS signal, associated with the formation ($E_\lambda \varphi_1$, ●) and decay ($E_\lambda \varphi_2$, ○) of the MLCT state of Ru(bpy)(CN) $_4^{2-}$ vs $(c_p \rho / \beta)_{RM}$ with *n*-alkanes (from left to right: *n*-hexane, *n*-heptane, *n*-octane, *n*-nonane, *n*-decane, *n*-undecane and *n*-dodecane) at $R = 5$ and 10.

that this decay is faster than the time resolution of the experiment. Fixing this parameter at any value between 1 fs and 1 ns always resulted in a similar value of the associated amplitude of the process. This amplitude φ_1 can thus be considered to be a reliable measure of the “prompt” processes.

In deoxygenated solutions and in the absence of quencher molecules, after laser excitation of Ru(bpy)(CN) $_4^{2-}$ only two consecutive processes occur: the formation of the triplet MLCT state followed by its decay to the ground state. Since for the Ru(bpy)(CN) $_4^{2-}$ complex the formation of the MLCT state is a prompt process with efficiency close to unity ($\Phi_R \approx 1$),¹¹ the amplitude φ_1 associated with the fast processes in the LIOAS signal is a measure of the MLCT formation, whereas the second amplitude and its respective decay time are assigned to the MLCT decay.¹ The value of τ_2 depended on the R value and did not depend on the external alkane solvent. The average values of τ_2 in AOT microemulsions are presented in Table 1 as a function of R . They decreased with R , and in every case they were longer than 100 ns, *i.e.*, the reported decay time for the MLCT state of Ru(bpy)(CN) $_4^{2-}$ in deoxygenated water.²¹ The fact that $\varphi_1 + \varphi_2 = 1 \pm 0.05$ indicates that all excited MLCT species return to the ground state.

For all R studied, the plots of $E_\lambda \varphi_1$ or $E_\lambda \varphi_2$ vs $(c_p \rho / \beta)_{RM}$ were linear as predicted by eq 1. In Figure 6 the data are shown for

$R = 5$ and $= 10$. The intercept (q_1) of the linear plots using φ_1 affords the enthalpy content of the MLCT state (eq 4)

$$\Delta H_{MLCT} = E_\lambda - q_1 \quad (4)$$

and the slope yields the structural volume change ΔV_R involved in the formation of the MLCT state (eq 1). Similarly, from the slope of the plot of eq 1 with φ_2 the value of ΔV_R associated with the decay of the MLCT state is obtained. Since Ru(bpy)(CN) $_4^{2-}$ has a low fluorescence quantum yield,²¹ the amount of energy lost by radiation ($E_{em} \Phi_{em} < 2$ kJ/mol) is negligible compared to the exciting energy E_λ . In this case, the intercept q_2 yields directly the value of ΔH_{MLCT} .

The values of ΔV_R for the formation and decay, the lifetimes, and the ΔH_{MLCT} of the MLCT of Ru(bpy)(CN) $_4^{2-}$ in AOT reverse micelles at various R values are listed in Table 1. ΔV_R increases up to $R = 10$, whereas ΔH_{MLCT} does not depend on the R value.

Temperature-dependent LIOAS measurements with Ru(bpy)(CN) $_4^{2-}$ in water, using Ni(ClO $_4$) $_2$ as calorimetric reference, afforded values of ΔV_R and ΔH_{MLCT} (Table 1) similar to those previously reported in water¹ using other calorimetric references and to the data in AOT microemulsions at $R > 10$. Figure 7 depicts the results of LIOAS measurements with Ru(bpy)(CN) $_4^{2-}$ in AOT microemulsions at $R = 20$ in various alkanes together with the temperature-dependent measurements in water. The values of ΔH_{MLCT} (obtained from the intercept) and of ΔV_R (obtained from the slope) are 1 order of magnitude more accurate than the data determined just in water (Table 1).

Discussion

The similar absorption spectrum and emission maximum in AOT dispersion and in water solutions confirm the initial assumption that Ru(bpy)(CN) $_4^{2-}$ should be localized in the core of the water pool of the AOT micelles. However, since the properties of the water pool such as viscosity and polarity significantly depend on R ,^{4,10} the lack of spectral shifts in AOT dispersions can only be a consequence of the extreme water affinity of the complex,^{11,27} *i.e.*, the second-sphere donor–acceptor interactions of the cyanides with water inside the water pool should be identical to those in neat water. This conclusion is also supported with the fact that the ΔH_{MLCT} value does not change with R , and it is the same as the energy of the emission band onset of Ru(bpy)(CN) $_4^{2-}$ at 25 °C.¹

In spite of the lack of spectral shifts, the increase in the emission quantum yield and in the decay lifetimes at lower R values (Table 1) indicate changes in the microenvironment of the probe. In fact, Φ_{em} correlates linearly with τ_2 , indicating that the unimolecular rate constant for radiation deactivation does not change. Thus, the radiationless deactivation process

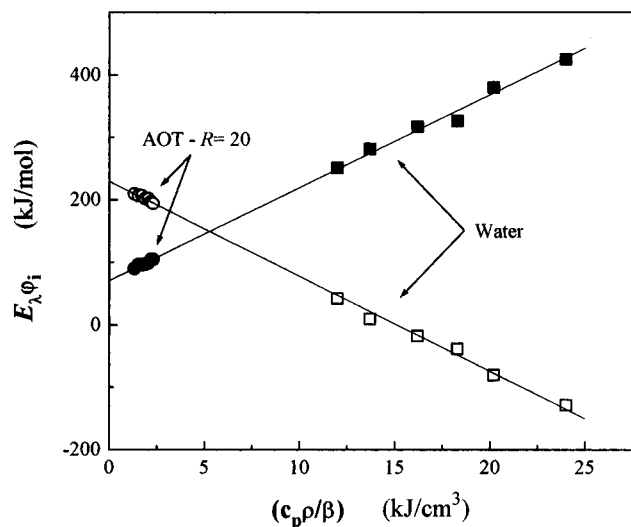


Figure 7. First and second amplitudes of the fitting function for the LIOAS signal, associated with the formation ($E_{\lambda\phi_1}$, filled symbols) and decay ($E_{\lambda\phi_2}$, open symbols) of the MLCT state of $\text{Ru}(\text{bpy})(\text{CN})_4^{2-}$, vs $(c_p \rho / \beta)$ of the medium, in water solutions (squares, from left to right: 35, 30, 25, 22, 20, and 17 °C) together with the data for AOT reverse micelles solutions in *n*-alkanes (circles from left to right: *n*-hexane, *n*-heptane, *n*-octane, *n*-nonane, *n*-undecane, and *n*-dodecane) at $R = 20$. The measurements in AOT-*n*-dodecane at $R = 20$ were carried out at 18 °C, due to the instability of the reverse micelles at 25 °C.

is affected by a decrease of the acceptor modes, possibly due to the rigidity of the water molecules that at low R values are attached to the polar head groups of the surfactant. Recently, similar features have been observed for $\text{Ru}(\text{bpy})(\text{CN})_4^{2-}$ upon formation of an adduct with the [32]ane $\text{N}_8\text{H}_8^{8+}$ polyaza macrocycle in water.²⁸

The value of ΔV_R for the MLCT formation and decay in AOT reverse micelles (Table 1) is also explained on the basis of interactions between $\text{Ru}(\text{bpy})(\text{CN})_4^{2-}$ and the water molecules of the first solvation shell.¹ In short, upon MLCT excitation, the change in the oxidation state from Ru(II) to Ru(III) is accompanied by a strong reduction in the π back-bonding and by a shift in electron density from the cyanide ligands to the central metal. Thus, the hydrogen bonds to the water molecules are expected to be weakened, resulting in an expansion of the whole system. In turn, when the MLCT state decays, the opposite effect occurs and a contraction of the same magnitude is observed.¹

In AOT microemulsions at $R < 10$, the ΔV_R value is significantly smaller (Table 1). This difference is explained on the basis of the structure of the water pool. At low R values the water molecules in the micellar core can be considered "bound" or associated with the polar head groups and the sodium counterions of the surfactant.⁴⁻⁸ Thus, in the MLCT state the displacement of the water-bonding molecules moving away from the cyanide ligand is hindered, probably due to the higher viscosity of the water pool allowing for a smaller expansion. As R increases, the proportion of "free" water molecules present in the core of the water pool increases until the water environment resembles that of bulk water ($R \geq 10$) and the ΔV_R in AOT solutions is similar to the value in neat water (Table 1). The above results are in agreement with the strong reduction with R of the relaxation time of the water molecules inside AOT reverse micelles (from 8 ns at $R = 4$ to 1.7 ns at $R = 32$).²⁹

The presence of the two types of water inside reverse micelles is clearly demonstrated by the variation of τ_2 and of ΔV_R for the formation of the MLCT state with R (Figure 8). Two regions are distinguished, one with a large slope at $R < 10$ and the

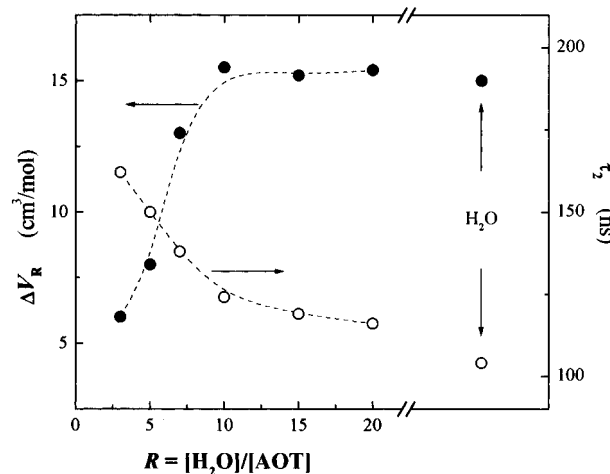


Figure 8. Decay lifetime (τ_2) and structural volume change (ΔV_R) associated with the formation of the MLCT state of $\text{Ru}(\text{bpy})(\text{CN})_4^{2-}$ in 0.1 M AOT-*n*-alkanes reverse micelles at various R values.

other one with a small slope at larger R . Thus, $\text{Ru}(\text{bpy})(\text{CN})_4^{2-}$ probes changes of the water pool properties. A similar dependence with R , albeit through the sensing of the interface properties, has been observed for the decay lifetime of exciplexes formed between pyrene derivatives and *N,N*-dimethylaniline in AOT microemulsions.³⁰

Since the water pool properties at large R values resemble those of bulk water, LIOAS measurements in reverse micelles at high R values dispersed in a series of organic solvents can be used in combination with temperature-dependent measurements in neat water, in order to expand the range of the $(c_p \rho / \beta)$ ratio (Figure 7). This combination of data affords a higher accuracy of the ΔV_R and ΔH_{MLCT} values derived using eq 1, especially of the enthalpy values (see Table 1).

A similar approach was used when combining LIOAS measurements in alkanes with temperature-dependent measurements in aqueous micelles for a photoreaction occurring in a lipophilic medium.¹⁸ The fact that the combination of data affords compatible data validates the procedures used for the calculation of the thermoelastic parameters of the microheterogeneous media and the applicability of this approach.

Conclusions

The structural volume change, ΔV_R , associated with the MLCT formation of $\text{Ru}(\text{bpy})(\text{CN})_4^{2-}$, as well as the emission quantum yields and lifetimes, determined in AOT reverse micelles in *n*-alkanes at 25 °C, reveals the ability of this complex to probe the water structure inside the micelles. Thus, at high R values the behavior is like in homogeneous water solution, while at low R values the rigidity of the water core is reflected in a much smaller expansion and somewhat higher emission lifetime and quantum yield. The results underline the weight of specific solvation effects, such as the second-sphere solvent interactions in the values of the photoinduced transient volume changes measured by photothermal techniques, particularly in aqueous media.

However, the possibility of using the complex studied in this work for the sensing of the type of water in complex systems, such as biological samples, is limited by its high reactivity, particularly as a powerful photoinduced electron donor.

The ΔV_R values for the water-soluble complex depend only on the aqueous microenvironment sensed by the complex and not on the global composition of the solution. The external organic medium just amplifies the pressure pulse generated in the core of the reverse micelle. This fact led to the strategy of

combining the temperature-dependent data in neat water with the data for the complex inside the water pool of micelles dispersed in various *n*-alkanes at high *R* values in order to expand the range of ($c_p\rho/\beta$) values. This strategy affords a higher accuracy in the values of ΔV_R and ΔH for the photo-produced species, in this case the MLCT state of the complex, and may find application in the future to the study of various types of reactions occurring in aqueous medium.

Acknowledgment. The able technical assistance of Dagmar Lenk and Sigi Pörting is gratefully acknowledged. We thank Dr. Maria Teresa Indelli and Professor Franco Scandola (University of Ferrara) for the sample of Ru(CN)₄K₂. We are indebted to Professor Kurt Schaffner for his continuous and generous support and interest.

References and Notes

- (1) Habib Jiwan, J. L.; Wegewijs, B.; Indelli, M. T.; Scandola, F.; Braslavsky, S. E. *Recl. Trav. Chim. Pays-Bas* **1995**, *114*, 542–548.
- (2) Gensch, T.; Braslavsky, S. E. *J. Phys. Chem. B* **1997**, *101*, 101–108.
- (3) Braslavsky, S. E.; Heibel, G. E. *Chem. Rev.* **1992**, *92*, 1381–1410.
- (4) Luisi, P. L.; Straub, B. E., Eds. *Reverse Micelles*; Plenum Press: New York, 1984.
- (5) Pileni, M. P., Ed. *Structure and Reactivity in Reverse Micelles*; Elsevier: Amsterdam, 1989.
- (6) Zinsli, P. E. *J. Phys. Chem.* **1979**, *83*, 3223–3231.
- (7) Wong, M.; Thomas, J. K.; Grätzel, M. *J. Am. Chem. Soc.* **1976**, *98*, 2391–2397.
- (8) Keh, E.; Valeur, B. *J. Colloid Interface Sci.* **1981**, *79*, 465–478.
- (9) Lissi, E. A.; Encinas, M. V.; Bertolotti, S. G.; Cosa, J. J.; Previtali, C. M. *Photochem. Photobiol.* **1990**, *51*, 53–58.
- (10) Encinas, M. V.; Lissi, E. A.; Bertolotti, S. G.; Cossa, J. J.; Previtali, C. M. *Photochem. Photobiol.* **1990**, *52*, 981–986.
- (11) Scandola, F.; Indelli, M. T. *Pure Appl. Chem.* **1988**, *60*, 973–980.
- (12) Callis, J. B.; Parson, W. W.; Gouterman, M. *Biochim. Biophys. Acta* **1972**, *267*, 348–362.
- (13) Habib Jiwan, J. L.; Chibisov, A. K.; Braslavsky, S. E. *J. Phys. Chem.* **1995**, *99*, 10246–10250.
- (14) Hung, R. R.; Grabowski, J. J. *J. Am. Chem. Soc.* **1992**, *114*, 351–353.
- (15) Morais, J.; Zimmt, M. B. *J. Phys. Chem.* **1995**, *99*, 8863–8871.
- (16) Wegewijs, B.; Verhoeven, J. W.; Braslavsky, S. E. *J. Phys. Chem.* **1996**, *100*, 8890–8894.
- (17) Herman, M. S.; Goodman, J. L. *J. Am. Chem. Soc.* **1989**, *111*, 1849–1854.
- (18) Schmidt, R.; Schütz, M. *Chem. Phys. Lett.* **1996**, *263*, 795–802.
- (19) Lang, J.; Jada, A.; Malliaris, A. *J. Phys. Chem.* **1988**, *92*, 1946–1953.
- (20) Redmond, R. W. *Photochem. Photobiol.* **1991**, *54*, 547–556.
- (21) Bignozzi, C. A.; Chiorboli, C.; Indelli, M. T.; Rampi Scandola, M. A.; Varani, G.; Scandola, F. *J. Am. Chem. Soc.* **1986**, *108*, 7872–7873.
- (22) Churio, M. S.; Angermund, K.; Braslavsky, S. E. *J. Phys. Chem.* **1994**, *98*, 1776–1782.
- (23) Riddick, J. A.; Bunger, W. B.; Sakano, T. K., Eds. *Organic Solvents*; John Wiley: New York, 1986.
- (24) Terazima, M. *J. Chem. Phys.* **1996**, *105*, 6587–6597.
- (25) Cao, Y. N.; Chen, H. X.; Diebold, G. J. Sun, T.; Zimmt, M. B. *J. Phys. Chem. B* **1997**, *101*, 3005–3011.
- (26) Owen, B. B.; Simons, H. L. *J. Phys. Chem.* **1957**, *61*, 479–482.
- (27) Timpson, C. J.; Bignozzi, C. A.; Sullivan, B. P.; Kober, E. M.; Meyer, T. J. *J. Phys. Chem.* **1996**, *100*, 2915–2925.
- (28) Rampi, M. A.; Indelli, M. T.; Scandola, F.; Pina, F.; Parola, J. *Inorg. Chem.* **1996**, *35*, 3355–3361.
- (29) Sarkar, N.; Das, K.; Datta, A.; Das, S.; Bhattacharyya, K. *J. Phys. Chem.* **1996**, *100*, 10523–10527.
- (30) Borsarelli, C. D.; Cosa, J. J.; Previtali, C. M. *Langmuir* **1992**, *8*, 1070–1075.